ARTICLE

Influence of the Polymer Backbone Structure on the Properties of Aromatic Ionomers with Pendant Sulfobenzoyl Side Chains for Use As Proton-Exchange Membranes

Elin Persson Jutemar and Patric Jannasch*

Polymer & Materials Chemistry, Department of Chemistry, Lund University, P.O. Box 124, SE-221 00 Lund, Sweden

ABSTRACT Six different ionomers having various aromatic polymer backbones with pendant 2-sulfobenzoyl side chains were prepared by nucleophilic aromatic substitution reactions of lithium 2,6-difluoro-2′-sulfobenzophenone with 4,4-biphenol, 2,7-dihydroxynaphthalene, 4,4-isopropylidenediphenol, 4,4-dihydroxydiphenyl ether, 4,4′-thiodiphenol, and 4,4′-thiobisbenzenethiol, respectively, to produce four poly(arylene ether)s, one poly(arylene ether sulfide), and one poly(arylene sulfide). Mechanically tough proton-exchange membranes with ion-exchange capacities in the narrow range from 1.9 to 2.3 mequiv/g were cast from the high-molecular-weight ionomers, and subsequently investigated with respect to their structure−property relationships. Glass transitions were only detected for ionomers in the sodium salt form, and increasing glass-transition temperatures (T_g) were found to give higher thermal decomposition temperatures. Analysis by small-angle X-ray scattering indicated that the ionic clustering was promoted for ionomers with flexible polymer backbones and low T_g values. The proton conductivity of the membranes at 80 °C under fully humidified conditions was found between 0.02 and 0.2 S/cm and appeared to depend primarily on the T_g.

KEYWORDS: polyaromatics • polycondensations • sulfonated polymer electrolytes • proton-exchange membrane fuel cells • SAXS

INTRODUCTION

Proton-exchange membrane fuel cells (PEMFC)s are increasingly regarded as promising environmentally benign power sources (1, 2). Today, intensive development is directed toward reducing the cost and increasing the durability and performance to expand the operating window of PEMFC systems for a range of different applications. Proton-exchange membranes based on sulfonated polymers in the protonated state are key fuel cell components that need to be developed further to meet the demands from industry. The state-of-art membranes currently include perfluorosulfonic acid membranes such as Nafion, which offer satisfactory fuel cell performance below 90 °C, as long as the degree of humidification is sufficient (3). However, at higher temperatures, Nafion suffers from poor mechanical properties and loss of proton conductivity (4). These shortcomings have driven an intensive research toward new alternative ionomers (5−7). In this respect, sulfonated aromatic hydrocarbon polymers such as poly(arylene ether sulfone)s, poly(arylene ether ketone)s and poly(phenylene)s have shown attractive properties due to their high thermal and chemical stability combined with good mechanical properties (6, 8−10).

Well-designed sulfonated aromatic polymers characteristically have a balanced composition of hydrophilic and hydrophobic segments. When a proton-exchange membrane has absorbed a sufficient amount of water, these segments phase separate to form a hydrophobic polymer-rich phase domain and a percolating hydrophilic network of nanopores containing the water. In these nanopores, the water dissociates the acid units and functions as the proton solvent to facilitate the transport of the protons. The viscoelastic property of the hydrophobic phase ensures the mechanical strength and dimensional stability of the membrane during PEMFC operation. The properties of the membrane are, however, highly dependent on the nature of both the hydrophobic and the hydrophilic phase domain. One of the main challenges is to find macromolecular structures and combinations of hydrophilic and hydrophobic segments that will give the overall best combination of membrane properties (11, 12).

Several investigations have shown that aromatic ionomers with sulfonic acid units statistically placed along the backbone polymer typically develop quite inefficient ionic networks for proton transport, leading to low conductivities in comparison to Nafion (13, 14). This is probably at least due to weaker phase segregation and a rather poor ability to form ionic cluster because of the stiffer and less hydrophobic character of the polymer backbone in relation with that of Nafion (15). Moreover, the sulfonic acid units of the aromatic ionomers have a lower acidity and are generally not placed on side chains as those of Nafion (15). The conductivity of aromatic ionomers may however be raised to the same level as Nafion simply by increasing the degree of sulfonation. Unfortunately, this strategy results in exces-

* Corresponding author. E-mail: patric.jannasch@polymat.lth.se. Tel: +46 462229860. Fax: +46 462224012.
Received for review September 10, 2010 and accepted November 16, 2010

DOI: 10.1021/am1008612

Published on Web 12/07/2010

sive water uptake and the loss of the mechanical integrity of the membrane (16).

Different promising approaches have been developed to enhance the properties of sulfonated aromatic hydrocarbon membranes by concentrating the sulfonic acid groups to specific chains segments in the polymer (17). By increasing the phase separation, this concept allows for the formation of a membrane morphology that will restrict the water uptake and swelling of the sulfonated hydrophilic phase domain. One of the approaches is to locate the sulfonic acid groups on side chains grafted onto the polymer backbone, similarly to Nafion. Using this strategy, various aromatic ionomers with sulfonated aromatic (18−22), alkyl (23, 24), aromatic-alkyl (25), and perfluoroalkyl (26) side chains have been prepared and investigated. Another successful strategy is to concentrate the sulfonic acid groups to specific blocks in the backbone polymer. Thus, various sulfonated and nonsulfonated oligomers with reactive chain ends have been coupled together to form a wide range of different hydrophilic−hydrophobic multiblock copolymers (27−29). Although these copolymers show an enhanced performance in relation to sulfonated homopolymers and statistical copolymers, the latter two polymer classes are still the ones primarily being used in PEMFCs, especially by the industry. The reason is the larger number of available synthetic routes and the ease of preparation in comparison with the usually very complex methods required for the block copolymers.

Recently, we reported on the synthesis and polymerization of a new monomer 2,6-difluoro-2′-sulfobenzophenone (DFSBP) (30). The lithium salt of this monomer was synthesized in one pot by reacting 2,6-difluorophenyllithium with 2-sulfobenzoic acid cyclic anhydride in THF at −70 °C, whereafter the product conveniently crystallized out of solution. Polymerizations of DFSBP in nucleophilic aromatic substitution reactions with, e.g., suitable diols give ionomers with pendant 2-sulfobenzoyl side chains. In the present study, the influence of the polymer backbone structure on the properties of aromatic ionomers prepared using DFSBP was studied. Consequently, a series of ionomers comprising four poly(arylene ether)s, one poly(arylene ether sulfide), and one poly(arylene sulfide), all within a narrow ion-exchange capacity range, was synthesized via polycondensation reactions with DFSBP in combination with different diols and a dithiol in order to vary the backbone structure. Important membrane properties, such as ionic clustering, water uptake, proton conductivity, and thermal properties, were investigated and correlated to the nature of the polymer backbone.

EXPERIMENTAL SECTION

Materials. The lithium salt of DFSBP was prepared by reacting 2,6-difluorophenyllithium with 2-sulfobenzoic acid cyclic anhydride in THF at −70 °C, as previously described in detail (30). The product was then purified by recrystallization from methanol. Potassium carbonate (Acrôs, 99+%) was dried at 120 °C overnight before use. 4,4-Biphenol (Acrôs, 97%) was recrystallized from ethanol; 4,4′-thiodiphenol (Sigma-Aldrich, 99%), 4,4-isopropylidenediphenol (bisphenol A, Acrôs, 97%), and 4,4′-thiobisbenzenethiol (TBBT, Sigma-Aldrich, 98%) were recrystallized from toluene; 4,4-dihydroxydiphenyl ether (TCI Europe, >98%) was recrystallized from a 50/50 v/v methanol/water mixture; and 2,7-dihydroxynaphthalene (TCI Europe, >99%) was recrystallized from water before being dried in vacuo at 80 °C overnight. *N*,*N*-Dimethylacetamide (DMAc, Acrôs, 99%), toluene (Fisher Scientific, HPLC grade), cyclohexane (Sigma-Aldrich, HPLC grade), 2-propanol (IPA, Fisher Scientific, HPLC grade), and *N*-methylpyrrolidone (NMP, Acrôs, 99%) were all used as received. A backbone sulfonated polysulfone (PSU) with an IEC of 1.76 mequiv/g was prepared following the method described by Kerres et al. (31).

Polycondensations. Six different ionomers were synthesized by nucleophilic aromatic substitution reactions involving DFSBP, as outlined in Scheme 1. The synthesis of the poly(arylene sulfide) (PAS) has been described previously (30). The other five ionomers were prepared in a similar way from equimolar amounts of DFSBP and various diols. In a typical procedure, using the preparation of PAE1 as an example, 4,4-biphenol (0.3094 g, 1.662 mmol), DFSBP (0.5055 g, 1.662 mmol), and K_2CO_3 (0.287 g, 2.08 mmol) were added to a mixture of DMAc (4 mL) and toluene (4 mL) in a two-necked flask equipped with a magnetic stirrer, a nitrogen inlet, and a Dean−Stark trap with a condenser having an outlet fitted with a calcium chloride filter. The reaction mixture was first heated to 160 °C for 4 h. After dehydration and removal of the toluene, the reaction temperature was raised to 175 °C, and kept at this temperature until the ionomer precipitated. This occurred after 1 h for PAE2, after 2 h for PAE1, PAE3, and PAEES, and after 3 h for PAE4. The reaction temperature was then lowered until the respective polymer regained solubility, which occurred at 110 °C for PAE2, at 100 °C for PAE4, and at room temperature for PAE1, PAE3, and PAEES. The reaction mixtures were kept at these respective temperatures for 15 h before precipitation of the ionomers in an excess of IPA at room temperature. The precipitates of all ionomers, except for PAE1, were filtered and washed repeatedly with fresh IPA and water. After drying, the products were redissolved in DMAc and the same purification procedure was repeated once more from a more dilute solution. Ionomer PAE1 was found to be nearly water-soluble after washing with IPA and the precipitate was therefore first dried in vacuo at 80 °C. Next, a water insoluble film of PAE1 was cast from an NMP solution, followed by leaching in distilled water. Finally, all ionomers were dried in vacuo at 80 °C for 24 h.

Ionomer Characterization. ^{1}H NMR data were collected using a Bruker DRX400 spectrometer. Spectra were recorded at 400.13 MHz and the chemical shifts are reported relative to DMSO-d_6 (δ 2.50 ppm). The intrinsic viscosity ([η]) of the ionomers was measured by using an Ostwald capillary viscometer in a thermostatted water bath at 25 °C. The samples were dissolved in a 0.05 M solution of LiBr in DMSO and were analyzed in the concentration range 0.7−10.1 g/L.

Membrane Preparation. Membranes of the ionomers were cast in their potassium salt form from 5 wt % solutions in NMP. All solutions were passed through 0.45 μm porous PTFE filters before membrane casting in Petri dishes under N_2 flow at 120 °C for 24 h, followed by drying in vacuo at 80 °C for 24 h. Membranes with a thickness of 70−160 μm were ion-exchanged to the protonated form by immersion in 1 M aqueous HCl for 2 days, followed by leaching with distilled water for 2 days, during which time the water was exchanged several times.

Thermal Characterization. A Q1000 calorimeter from TA Instruments was used to carry out the differential scanning calorimetry (DSC) investigations. During the DSC experiment, the polymers were first heated to 400 °C, or alternatively to 10 °C below T_d if this temperature was below 410 °C. The samples were then cooled to 50 °C, followed by heating to 400 °C. All heating and cooling rates were kept at 10 °C/min. Glass-

Scheme 1. Synthetic Pathway to the Various Ionomers via Potassium Carbonate Mediated Nucleophilic Aromatic Substitution Reactions

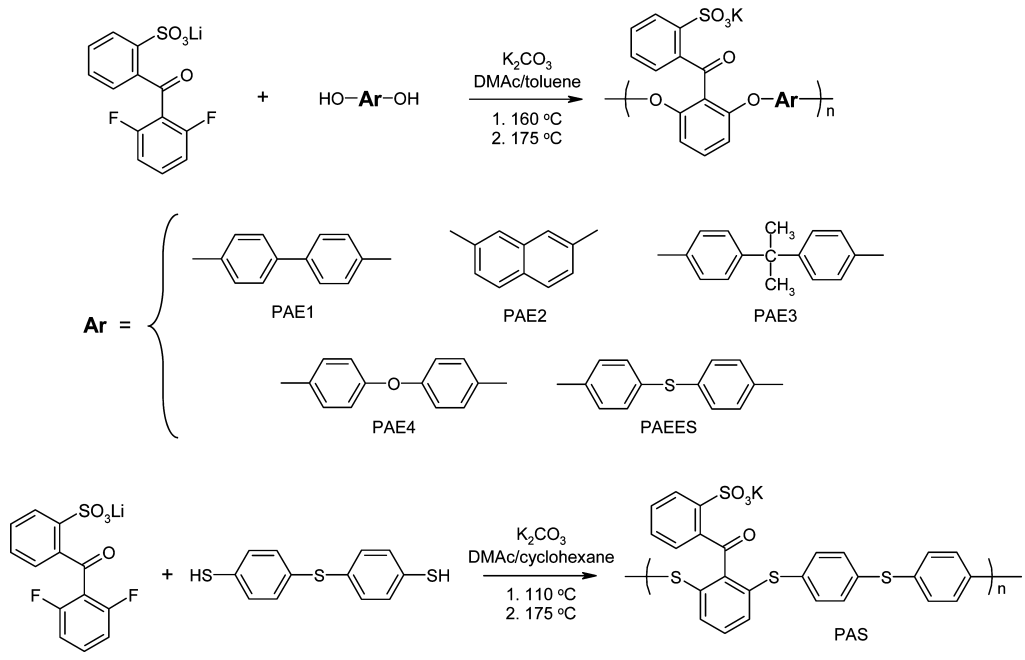

transition temperatures (T_g) were taken as the midpoint of the transition recorded during the second heating scan.

The thermal stability was evaluated by thermogravimetric analysis (TGA) using a Q500 analyzer from TA Instruments. The samples were analyzed, both in the protonated form and the sodium salt form, under N_2 during heating from 50 to 600 at 10 °C/min, as well as under air during heating from 50 to 600 at 1 °C/min. Prior to the heating scan, the samples were predried under N_2 at 150 °C for 10 min to remove water. The degradation temperature (T_d) was taken as the temperature at which the polymer had lost 5% of its original weight during the heating.

X-ray Scattering. SAXS measurements were carried out on membranes ion-exchanged to the Pb^{2+} form by immersion in a 1 wt % aqueous solution of lead acetate. The scattering experiments were performed on a Kratky compact small angle system equipped with a position sensitive wire detector with 1024 channels having a width of 53.6 μm. CuK_α radiation with a wavelength of $\lambda = 1.524$ Å was provided by a Seifert ID 3000 X-ray generator operating at 55 kV and 40 mA. Dry samples were placed between mica sheets in a sealed solid sample cell and the measurements were performed during 2 h at 25 °C. The wave vector (q) was calculated according to

$$q = 4\pi/\lambda \times \sin\theta \qquad (1)$$

where 2θ is the scattering angle. The characteristic separation length (d), i.e. the Bragg spacing, was calculated as

$$d = 2\pi/q \qquad (2)$$

Water Uptake and Ion-Exchange Capacity Measurements. The water uptake (w_{water}) was measured under immersed conditions after equilibration in distilled water for at least 48 h, and at 98% RH after storage in a sealed vessel with a saturated aqueous solution of $CuSO_4 \cdot 5H_2O$. To obtain the wet weight (W_{wet}), we gently removed the excess water with tissue paper before weighing the swollen membranes. The dry weight (W_{dry}) was obtained after drying under a vacuum at 80 °C overnight. The water uptake was then calculated as

$$w_{water} = (W_{wet} - W_{dry})/W_{dry} \times 100\% \qquad (3)$$

The ion-exchange capacity, IEC, was measured by titration of acidic membranes. Protonated membranes were soaked in an aqueous 2 M NaCl solution for at least 72 h. The solutions were titrated with a 0.01 M KOH solution using phenolphthalein as indicator.

The state of the water in the membranes was investigated via DSC by observing the endothermic peaks associated with water melting. The membranes were first allowed to equilibrate at room temperature in distilled water for at least 24 h. Excess water was carefully removed with tissue paper before placing the samples in a sealed Al container. In the DSC experiment, the samples were first cooled from 25 to −60 °C, and then kept at −60 °C for 3 min, before heating to 25 °C. The scan rate was 5 °C/min in all cases. The amount of freezing water was calculated by integrating the peak of the melt endotherm and comparing this value with the heat of fusion of pure ice, 334 J/g (32). By combining the calculated amount of freezing water and the gravimetrically determined total water absorption, the total number of water molecules per sulfonic acid group (λ) and the freezing number of water molecules per sulfonic acid group ($\lambda_{freezing}$) were determined.

Conductivity Measurements. Proton conductivity was evaluated by electrochemical impedance spectroscopy (EIS) using a Novocontrol high-resolution dielectric analyzer V 1.01S equipped with a Novocontrol temperature system. Impedance data was collected over the frequency range of 1×10^7 to 1×10^{-1} Hz at a voltage amplitude of 50 mV, and were analyzed using the software WinDeta from Novocontrol. Measurements were performed at 100% RH with the membranes pre-equilibrated at 98% RH. Samples were placed together with a small droplet of distilled water in the sealed two-probe measurement cell and the proton conductivity data of the membranes were recorded during heating from −20 to 120 °C, then during cooling to −20

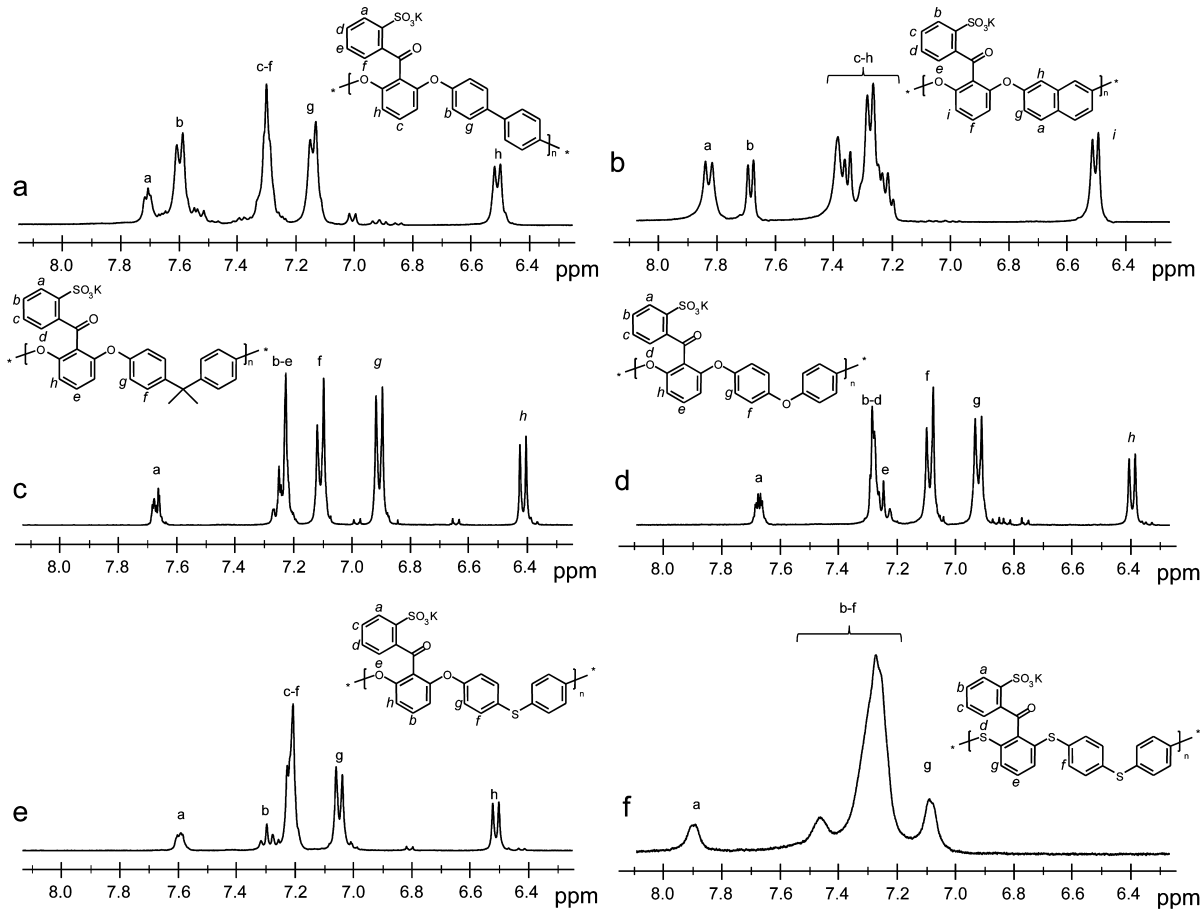

FIGURE 1. ^{1}H NMR spectra of the ionomers (a) PAE1, (b) PAE2, (c) PAE3, (d) PAE4, (e) PAEES, and (f) PAS. The data were collected using DMSO-d_6 solutions of the samples.

°C, and finally during heating to 100 °C. The reported data were collected during the second heating scan.

RESULTS AND DISCUSSION

Polymer Preparation and Characterization. Six different ionomers having various aromatic polymer backbones, but all with the same pendant 2-sulfobenzoyl side chains, were prepared by nucleophilic aromatic substitution reactions with the aim to study the influence of the ionomer backbone structure on the ionic clustering and properties of the membranes. Thus, DFSBP was polymerized via polycondensations with one dithiol and various diols to obtain four poly(arylene ether)s (PAE1−4), one poly(arylene ether ether sulfide) (PAEES), and one poly(arylene sulfide) (PAS) according to Scheme 1. DFSBP was charged in equimolar amounts to the diols and the dithiol, respectively, together with a 25% excess of potassium carbonate. During the 4 h dehydration step, the reactants slowly precipitated, but regained solubility when the toluene was boiled off during heating to 175 °C. At this temperature, the reaction solutions increased in viscosity and the polymerizations were continued until the polymer lost solubility, which occurred after 1−3 h. The reaction temperature was then decreased to a temperature at which the polymer regained solubility. The reactor was kept at this temperature for 15 h before isolation of the products.

Figure 1 shows the ^{1}H NMR spectra of the purified ionomers. For the PAE and PAEES ionomers, all aromatic shifts were found between $\delta = 6.3-7.9$ ppm. The signal arising from the proton next to the sulfonic acid group was in all cases found between $\delta = 7.6-7.7$ ppm, whereas the protons ortho-to-ether on the DFSBP residues gave rise to signals between $\delta = 6.4-6.5$ ppm. In the case of PAE3, the signal arising from the aliphatic isopropylidene link was observed at $\delta = 1.6$ ppm (not shown). The small shifts found in the spectra of PAE1, PAE3, PAE4, and PAEES between $\delta = 6.6-7.0$ may indicate the formation of limited amounts of cyclic products. For the PAS ionomer, all shifts were found between $\delta = 7.0-8.0$ ppm. Moreover, the broader signals observed in the spectrum of the PAS ionomer indicated a limited mobility in the DMSO-d_6. The integrals of the signals were in excellent agreement with the respective ionomer structures.

The intrinsic viscosities of the ionomers, measured with DMSO solutions, are listed in Table 1 and ranged from 0.33 to 0.84 dL g^{-1}. The highest intrinsic viscosities were found for the ionomers that were kept at a higher reaction temperature after precipitation in the reactor. This may indicate that the polymerization proceeded beyond the point of precipitation, or that the polymers with the highest solubility in the reactor mixture reached the highest molecular weights.

Thermal Properties. The ionomer structure was shown to have a profound impact on the T_g, as seen in Table 1. Glass transitions were only found for the membranes in the sodium salt form: no glass transitions were detected for the

Table 1. Sulfonated Ionomer Membrane Data

					Na^+ form			H^+ form		98% RH		immersed		
membrane	$[\eta]$ (dLg^{-1})	IEC[a] (mequiv/g)	q ($Å^{-1}$)	d (Å)	T_g (°C)	T_d (°C) under N_2[b]	T_d (°C) under air[c]	T_d (°C) under N_2[b]	T_d (°C) under air[c]	w_{water} (%)	λ	w_{water} (%)	λ	$\lambda_{freezing}$
PAE1	0.41	2.22 (2.25)	0.40	16	300	419	370	239	204	50	12	114	29	7
PAE2	0.84	2.25 (2.39)	0.40	16	n/d[e]	409	365	294	267	44	11	627	155	87
PAE3	0.33	1.95 (2.06)	0.36	18	230	396	352	259	224	31	9	127	36	1
PAE4	0.59	2.08 (2.17)	0.37	17	241	403	353	229	194	38	10	141	38	10
PAEES	0.33	1.99 (2.10)	0.36	17	220	390	352	243	201	41	11	100	28	1
PAS	0.59	1.87 (1.97)	0.34	19	252	412	364	267	235	39	12	73	22	1

[a] Measured by titration, theoretical values within parentheses. [b] Measured at 10 °C/min. [c] Measured at 1 °C/min. [e] n/d: not detected.

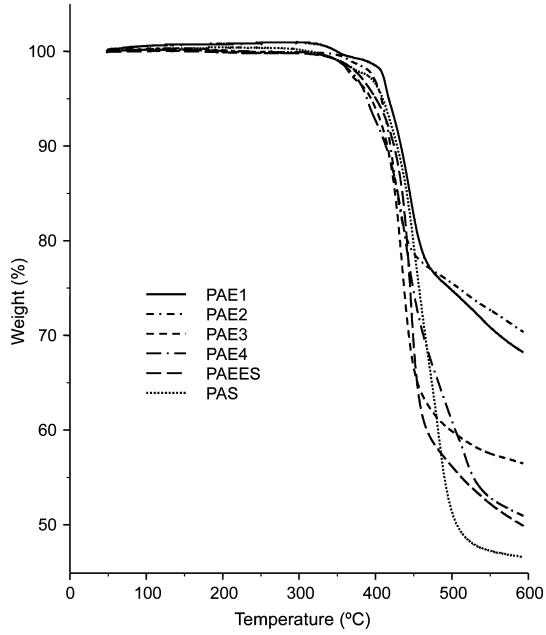

FIGURE 2. TGA traces of the ionomer membranes in the sodium salt form recorded under nitrogen at 10 °C/min.

membranes in the acid form. PAE3, PAE4, and PAEES with their quite flexible polymer backbones showed the lowest T_g values between 220 and 241 °C, whereas PAE1 and PAS with their less flexible backbones showed T_g values of up to 300 °C. PAE2, incorporating rigid naphthyl moieties, supposedly had a very high T_g because no glass transition was detected in the temperature range up to the onset of degradation at 400 °C. PSUs bearing 2-sulfobenzoyl side chains have previously been reported to have considerably lower T_g values than the present ionomers (22). However, this is most probably explained by the considerably lower IEC values of the PSU in that study.

The thermal stability of the ionomer membranes in both the sodium salt and the acid form was evaluated by TGA analysis. Measurements under air at 1 °C/min were undertaken to study the stability under oxidative conditions, and measurements under nitrogen at 10 °C/min were performed to study the degradation under less drastic conditions. Figure 2 shows the TGA traces of the ionomers in their sodium salt form when heated in nitrogen at 10 °C/min. All six ionomers showed a large weight loss when approaching approximately 400 °C, with values of T_d in the range between 390 and 419 °C. Notably, the highest T_d values were found among the ionomers with the highest T_g values. In contrast to the other membranes, the rate of the weight loss of the PAE1 and PAE2 ionomers leveled off after an initial loss of about 20 wt %, which corresponded to the weight of the sulfonic acid groups in these ionomers. This observation indicated a different degradation mechanism under nonoxidative conditions for PAE1 and PAE2, which had comparatively stiff backbones with a rather high degree of aromaticity, as compared to the other ionomers. In the acid form under air, ionomer PAE2 with the rigid naphthyl group in the polymer backbone displayed the highest thermal stability with T_d = 267 °C, whereas PAE4 showed the lowest thermal stability, with T_d = 194 °C, as seen in Table 1. In comparison, sulfonated PSUs have shown degradation temperatures between 220 and 280 °C under air at 1 (22), 5 (25), and 10 °C/min (33). As expected, the stability was higher under nitrogen than under air, and the ionomers in the acid form showed lower values of T_d than in the sodium salt form.

X-ray Scattering. The ability of the ionomers to phase separate by clustering of ionic groups was studied by SAXS. This technique allows the identification of the characteristic separation length between the ionic clusters in terms of the position (q value) and the width of the so-called ionomer peak (34). Before the measurements, the membranes were ion-exchanged to the Pb^{2+} form to increase the contrast between the ionic clusters and the hydrophobic polymer-rich domain.

The SAXS profiles of the six ionomers are shown in Figure 3, together with the corresponding profile of Nafion and a backbone sulfonated PSU with an IEC of 1.76 mequiv/g. The respective q values of the ionomer peaks and the corresponding characteristic separation lengths, d, are given in Table 1. As seen in Figure 3, Nafion gave rise to a rather sharp ionomer peak at q = 0.18 $Å^{-1}$, indicating a distinct and quite regular phase separation between the ion-rich domains and the hydrophobic polymer-rich domains with a characteristic separation length of d = 34 Å. The profile of the backbone sulfonated PSU showed a much broader ionomer peak shifted to a higher q value, as compared to the profile of Nafion. This indicated a smaller cluster separation, d = 23 Å, with a significantly wider distribution. The PSU main chain is far less hydrophobic and the sulfonic acid groups far less acidic than in Nafion, leading to less distinct ionic phase domains in the main chain sulfonated PSU

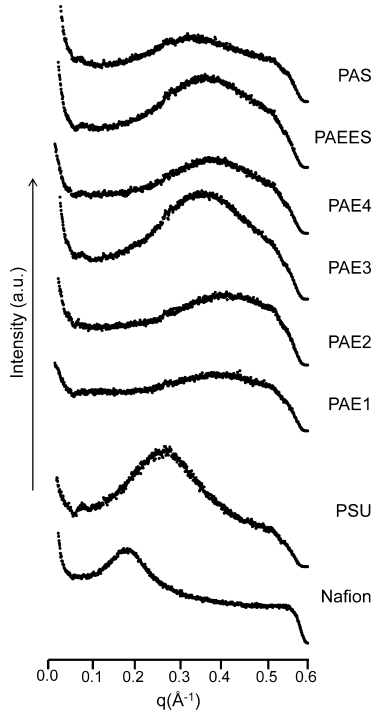

FIGURE 3. SAXS data recorded using dry ionomer membranes ion-exchanged with lead acetate.

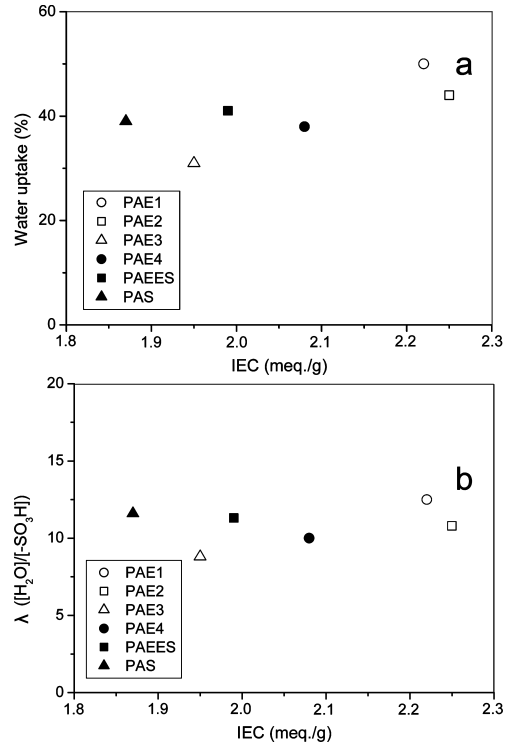

FIGURE 4. (a) Water uptake and (b) the corresponding λ-values of the ionomer membranes as a function of IEC after equilibration at RH 98% at 25 °C.

membranes. The six membranes based on the ionomers carrying sulfobenzoyl side chains clearly formed ionic clusters with ionomer peak positions corresponding to d = 16−19 Å. Although the widths of the ionomer peaks were quite similar, the position of the peaks differed greatly between the polymers bearing the sulfobenzoyl side chains and the backbone sulfonated PSU. Thus, the characteristic separation length between the ionic clusters in the former membranes were significantly smaller than in the membrane based on backbone sulfonated aromatic ionomers (35−37), Nafion (34, 36, 38), or other aromatic polymers bearing sulfonated side chains (22, 39, 40).

PAE4, PAEES, and PAS may be viewed as an analogous series of ionomers with the main chain links of the repeating unit varying from three ether linkages, via two ether linkages and one sulfide linkage, to three sulfide linkages, respectively. As seen in Figure 3, there is a tendency that the q values shifted to lower q values when the number of sulfide linkages increased, indicating larger characteristic separation lengths between the ionic clusters in the ionomers with sulfide linkages. Furthermore, out of these three ionomers, PAEES gave rise to the most pronounced ionomer peak.

For the present ionomers, which all had rather similar IEC values, the T_g seemingly had an influence on the SAXS profiles. This was demonstrated by a weaker ionic clustering of the PAE1, PAE2, and PAS ionomers. These three ionomers with high T_g values all had rather stiff links in their polymer backbones which, in relation to the other ionomers, apparently hindered the clustering of the ionic groups during membrane formation, possibly because of restricted chain mobility. In contrast, the PAE3, PAE4, and PAEES ionomers, with lower T_g values and more flexible polymer backbones, demonstrated a more pronounced ionic clustering.

PSUs functionalized with 2-sulfobenzoyl side chains have previously shown to give rise to very weak, hardly detectable, ionomer peaks. This has been explained by the position of the sulfonic acid group, ortho to the ketone link and close to the main chain, which may lead to decreased mobility and steric shielding of the individual acid units during membrane formation (22). The ionomer peaks of the membranes in this study demonstrated an improved ionic clustering, presumably because of the higher local chain flexibility around the sulfonated moieties. This apparently gave fewer restrictions in the clustering process. Yet, the ionomer peaks were still broad in comparison with the peak of Nafion.

Water Uptake Characteristics. The level of hydration of proton-exchange membranes is highly dependent on the IEC. However, at high levels of hydration the mechanical properties typically deteriorate due to the high degree of swelling. Consequently, the membrane properties should be tuned so that the water uptake is controlled and kept at a moderate level. Table 1 shows the water uptake data of the ionomer samples, and panels a and b in Figure 4 show the water uptake and λ-value (i.e., the number of water molecules per sulfonic acid group), respectively, as a function of IEC at 98% RH. As seen, the water uptake remained approximately constant with the IEC and ranged from 31 to 50 wt %, which corresponded to λ-values from 9 to 12. Most probably on the basis of its high IEC, the PAE1 membrane was found to have the highest water uptake.

Given the high IEC values of the membranes, the water uptake under immersed conditions was high, ranging from 73 to 627%, and was found to increase with increasing IEC,

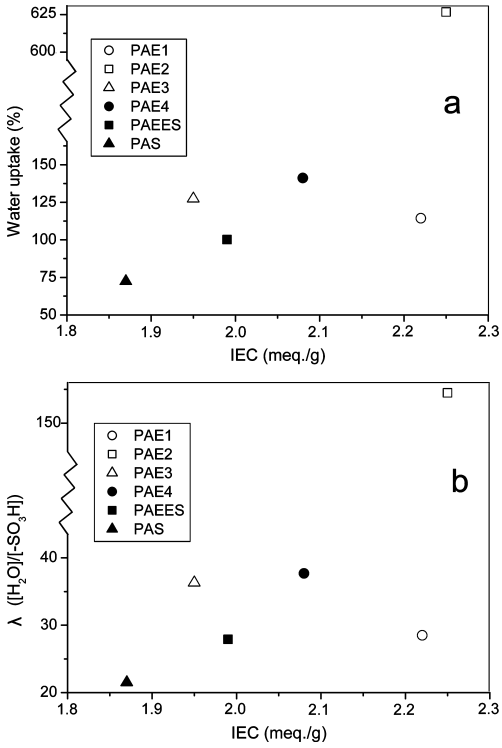

FIGURE 5. (a) Water uptake and (b) the corresponding λ-values of the ionomer membranes as a function of IEC after immersion in water at 25 °C.

as shown in Figure 5a. Membrane PAE1 was not water-soluble at room temperature, but dissolved at elevated temperatures. In contrast to the water uptake at 98% RH, membrane PAE1 had a lower water uptake under immersed conditions than expected from its high IEC. A possible explanation for this might be the comparatively stiff backbone polymer that gave rise to a high T_g, which in turn restricted the water uptake. In contrast to the situation at 98% RH, the rigid PAE2 was found to take up excessive amounts of water under immersed conditions. Moreover, the PAE2 membrane swelled unevenly, taking up much more water at the edges as compared to in the center of the membrane. This may possibly be due to an orientation of the ionomer chains during membrane formation. Further investigations are necessary to fully explain this behavior. The water uptake was found to increase with increasing IEC for the analogous series of PAE4, PAEES and PAS. This trend indicated that the IEC was the main factor determining the water uptake within this series under immersed conditions, rather than the polymer backbone structure. In Figure 5b, the λ-value is shown as a function of IEC. As expected, the λ-value showed similar trends as compared to the water uptake as a function of IEC, and ranged from 22 to 155.

On the basis of DSC measurements, the amount of freezable water in the membranes was determined under immersed conditions. The local environment of the water in the membrane can be identified from the temperature at which the water freezes. Nonfreezable water strongly interacts with sulfonic acid groups, whereas freezable water is "free", not intimately bound to the sulfonic acid groups. The tightly bound nonfreezable water has, under hydrated conditions, a critical influence on the depression of the T_g, which indirectly affects the proton conductivity (41, 42). The number of freezable water molecules per sulfonic acid group ($\lambda_{freezing}$) is presented in Table 1, showing that all the studied ionomers contained freezable water to some extent. In comparison, Nafion was found to have three freezable water molecules out of a total of 14 water molecules per sulfonic acid group. Expectedly, the PAE4 membrane contained moderate amounts of freezable water, whereas the highly swollen PAE2 membrane contained very large amounts of freezable water.

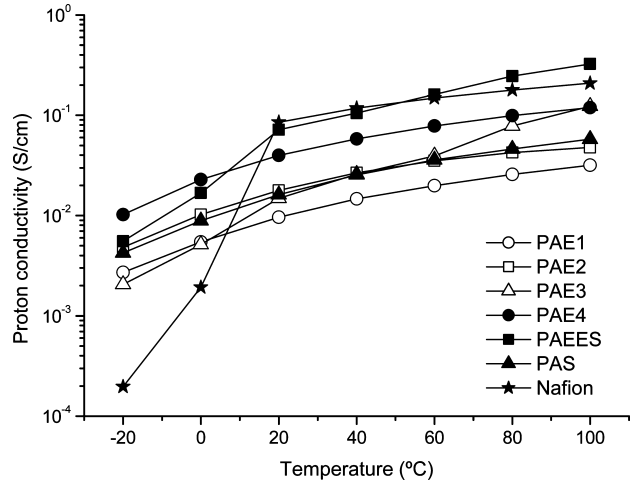

FIGURE 6. Proton conductivity plots for the ionomers with corresponding data for Nafion 117 for comparison. The data were measured by EIS with the membranes at 100% RH.

Proton Conductivity. The proton conductivity was measured by EIS during heating from −20 and 100 °C with the membranes at 100% RH in a sealed cell. Figure 6 shows that the conductivity of the membranes increased from −20 to 20 °C, especially for Nafion. Notably, the increase was the most pronounced for the membranes with the lowest T_g values; Nafion, PAE3 and PAEES. It is possible that these polymers increased their segmental mobility during the first heating cycle of the measurements to change conformation and induce a change in membrane morphology to accommodated increasing amounts of water. The "excess" water taken up by these membranes would be primarily freezing water−water, which led to sharply increasing proton conductivity below 0 °C as this water melted during heating. At subzero temperatures, all membranes had proton conductivities exceeding that of Nafion. Above 20 °C, the conductivity increased with approximately the same rate as a function of temperature. The slightly higher increase of membranes PAE3 and PAEES, with the conductivity of the latter membrane increasing further between 60 and 100 °C, may indicate a gradual change in morphology to accommodate increasing amounts of water. The aromatic membranes reached conductivities between 0.02 and 0.2 S/cm at 80 °C, with the PAEES membrane exceeding the conductivity of Nafion.

For the presently investigated ionomers, which all had rather similar IEC values and water absorption at 25 °C and 98% RH, there was a tendency that the T_g influenced the

proton conductivity. Thus, the lowest proton conductivities were found for the ionomers PAE1, PAE2, and PAS with stiff polymer backbones and high T_g values. The lower proton conductivities of these membranes were consistent with the less efficient ionic clustering in these membranes as observed by SAXS. Their high T_g values presumably lowered the mobility and degree of freedom during the membrane formation process when the ionomer was in solution or in a solvent-swollen state, thus hindering a strong segregation and leading to a rather poor ionic clustering (15). Within the analogous series of ionomers with different combinations of ether and sulfide linkages, the PAEES membrane reached the highest proton conductivity, followed by the PAE4 and the PAS membranes, an order that was correlated to the order of their T_g (Table 1). Thus, at the measurement conditions employed, the structure and stiffness of the polymer backbone, rather than the IEC and the water uptake, was found to influence the level of proton conductivity reached by the ionomers.

CONCLUSIONS

The variations in properties and ionic clustering were investigated for aromatic ionomers with different backbones functionalized with sulfobenzoyl side chains. Four poly(arylene ether)s, one poly(arylene ether sulfide), and one poly(arylene sulfide) with different backbone structures and stiffness's were successfully synthesized via nucleophilic aromatic substitution reactions involving the lithium salt of 2,6-difluoro-2′-sulfobenzophenone and various comonomers. Membranes cast from NMP solutions showed proton conductivities in the range of 0.02−0.2 S/cm under fully humidified conditions at 80 °C. There was a trend among the ionomers that the T_g of the backbone influenced the ionic clustering during membrane casting, which in turn influenced the proton conductivity reached by the membranes at 100% RH. Accordingly, the SAXS measurements showed that the ionic clustering was promoted by ionomers with flexible backbones and low T_g values, resulting in higher proton conductivity. On the other hand, ionomers with higher T_g values showed lower proton conductivity, but possessed a higher thermal stability than the former ionomers. The water uptake under immersed conditions was found to increase with an increasing IEC to reach very high values. Consequently, in order to employ the present ionomers as proton-exchange membranes, restrictions in water uptake are required. This may for example be achieved by introducing cross-links, increasing the molecular weights, or by copolymerization with nonsulfonated monomers to decrease the IEC.

Acknowledgment. We thank the Swedish Foundation for Strategic Environmental Research, MISTRA, for financial support.

REFERENCES AND NOTES

(1) Hickner, M. A. *Mater. Today* **2010**, *13*, 34–41.
(2) de Bruijn, F. *Green Chem.* **2005**, *7*, 132–150.
(3) Steele, B. C. H.; Heinzel, A. *Nature* **2001**, *414*, 345–352.
(4) Casciola, M.; Alberti, G.; Sganappa, M.; Narducci, R. *J. Power Sources* **2006**, *162*, 141–145.
(5) Rusanov, A. L.; Kostoglodov, P. V.; Abadie, M. J. M.; Voytekunas, V. Y.; Likhachev, D. Y. *Adv. Polym. Sci.* **2008**, *216*, 125–155.
(6) Maier, G.; Meier-Haack, J, *Adv. Polym. Sci.* **2008**, *216*, 1–62.
(7) Jannasch, P. *Curr. Opin. Colloid Interface Sci.* **2003**, *8*, 96–102.
(8) Rozière, J.; Jones, D. J. *Annu. Rev. Mater. Res.* **2003**, *33*, 503–555.
(9) Higashihara, T.; Matsumoto, K.; Ueda, M. *Polymer* **2009**, *50*, 5341–5357.
(10) Iojoiu, C.; Sanchez, J.-Y. *High Perform. Polym.* **2009**, *21*, 673–692.
(11) Bae, B.; Miyatake, K.; Watanabe, M. *Macromolecules* **2009**, *42*, 1873–1880.
(12) Hickner, M. A.; Ghassemi, H.; Kim, Y. S.; Einsla, B. R.; McGrath, J. E. *Chem. Rev.* **2004**, *104*, 4587–4612.
(13) Park, H. B.; Shin, H.-S.; Lee, Y. M.; Rhim, J.-W. *J. Membr. Sci.* **2005**, *247*, 103–110.
(14) Dyck, A.; Fritsch, D.; Nunes, S. P. *J. Appl. Polym. Sci.* **2002**, *86*, 2820–2827.
(15) Kreuer, K. D. *J. Membr. Sci.* **2001**, *185*, 29–39.
(16) Kerres, J. A. *J. Membr. Sci.* **2001**, *185*, 3–27.
(17) Yang, Y.; Holdcroft, S. *Fuel Cells* **2005**, *5*, 171–186.
(18) Lafitte, B.; Karlsson, L. E.; Jannasch, P. *Macromol. Rapid Commun.* **2002**, *23*, 896–900.
(19) Lafitte, B.; Puchner, M.; Jannasch, P. *Macromol. Rapid Commun.* **2005**, *26*, 1464–1468.
(20) Lafitte, B.; Jannasch, P. *Adv. Funct. Mater.* **2007**, *17*, 2823–2834.
(21) Wang, L.; Xiang, S.; Zhu, G. *Chem. Lett.* **2009**, *38*, 1004–1005.
(22) Jutemar, E. P.; Jannasch, P. *J. Membr. Sci.* **2010**, *351*, 87–95.
(23) Karlsson, L. E.; Jannasch, P. *J. Membr. Sci.* **2004**, *230*, 61–70.
(24) Zhu, J.; Shao, K.; Zhang, G.; Zhao, C.; Zhang, Y.; Li, H.; Han, M.; Lin, H.; Xu, D.; Yu, H.; Na, H. *Polymer* **2010**, *51*, 3047–3053.
(25) Pang, J. H.; Zhang, H. B.; Li, X. F.; Wang, L. F.; Liu, B. J.; Jiang, Z. H. *J. Membr. Sci.* **2008**, *318*, 271–279.
(26) Mikami, T.; Miyatake, K.; Watanabe, M. *ACS Appl. Mater. Interfaces* **2010**, *2*, 1714–1721.
(27) Nakabayashi, K.; Higashihara, T.; Ueda, M. *J. Polym. Sci., Part A: Polym. Chem.* **2010**, *48*, 2757–2764.
(28) Lee, H.-S.; Roy, A.; Lane, O.; Lee, M.; McGrath, J. E. *J. Polym. Sci., Part A: Polym. Chem.* **2010**, *48*, 214–222.
(29) Shin, C. K.; Maier, G.; Andreaus, B.; Scherer, G. G. *J. Membr. Sci.* **2004**, *245*, 147–161.
(30) Jutemar, E. P.; Takamuku, S.; Jannasch, P. *Macromol. Rapid Commun.* **2010**, *31*, 1348–1353.
(31) Kerres, J.; Cui, W.; Reichle, S. *J. Polym. Sci., Part A: Polym. Chem.* **1996**, *34*, 2421–2438.
(32) Nakamura, K.; Hatakeyama, T.; Hatakeyama, H. *Polymer* **1983**, *24*, 871–876.
(33) Lufrano, F.; Gatto, I.; Staiti, P.; Antonucci, V.; Passalacqua, E. *Solid State Ionics* **2001**, *145*, 47–51.
(34) Gebel, G.; Diat, O. *Fuel Cells* **2005**, *5*, 261–276.
(35) Luu, D. X.; Cho, E.-B.; Han, O. H.; Kim, D. *J. Phys. Chem. B* **2009**, *113*, 10072–10076.
(36) Takimoto, N.; Wu, L.; Ohira, A.; Takeoka, Y.; Rikukawa, M. *Polymer* **2009**, *50*, 534–540.
(37) Barique, M. A.; Wu, L.; Takimoto, N.; Kidena, K.; Ohira, A. *J. Phys. Chem. B* **2009**, *113*, 15921–15927.
(38) Yang, B.; Manthiram, A. *J. Power Sources* **2006**, *153*, 29–35.
(39) Yoshimura, K.; Iwasaki, K. *Macromolecules* **2009**, *42*, 9302–9306.
(40) Miyatake, K.; Yasuda, T.; Hirai, M.; Nanasawa, M.; Watanabe, M. *J. Polym. Sci., Part A: Polym. Chem.* **2006**, *45*, 157–163.
(41) Siu, A.; Schmeisser, J.; Holdcroft, S. *J. Phys. Chem. B* **2006**, *110*, 6072–6080.
(42) Kim, Y. S.; Dong, L.; Hickner, M. A.; Glass, T. E.; McGrath, J. E. *Macromolecules* **2003**, *36*, 6281–6285.

AM1008612